

## LOCAL HEAT TRANSFER ON THE ENTRANCE SEGMENT OF A TUBE WITH A SHARP INLET EDGE.

### 1. NATURE AND BEHAVIOR OF HEAT TRANSFER INTENSITY EXTREMA

V. M. Legkii and V. A. Rogachev

UDC 536.542:532.542

*Experimental results on local heat transfer on the entrance segment of a round smooth tube with a sharp leading edge when  $Re_d = (13-110) \cdot 10^3$ ,  $X/d = 0.1-13$ , which support the previously proposed model for separated flow, are examined. It is shown that under separated flow conditions the usual sequence of flow transitions in a boundary layer for mixed nonseparated flows and  $Re_d > 10^4$  is still retained. Formulas are obtained for calculating local heat transfer coefficients on a segment where a laminar boundary layer occurs, including cross sections where these coefficients acquire extreme values.*

Local heat transfer on entrance segments of tubes and channels having a sharp inlet edge with an angle of  $90^\circ$  within the range of  $Re_d > 10^4$  and  $X/d < 15$  has been thoroughly studied, mainly with the aim of making corrections to the equations that govern the specific features of heat transfer under developed flow conditions. At the same time, because of difficulties associated with attaining acceptable measuring accuracy when the reduced lengths approach zero and existing concepts of the mechanism of flow separation behind a sharp edge as a phenomenon accompanied by rapid boundary layer turbulization, up to now some details of the distribution  $\alpha = f(X/d)$  of primary importance have not been traced or have not been interpreted correctly on physical grounds. For example, beyond a maximum of the local heat transfer coefficients at  $X/d < 1$ , where attachment is presumed, a second maximum is found in [1] at  $X/d = 3-5$ , although it is not as well-defined as the first one. The important question of a possible deep minimum of the heat transfer coefficients in a stagnation region that, as follows from [2], is adjacent to the entrance cross section remains open. Owing to the aforesaid, the present article deals with axial distributions of the local heat transfer coefficients in air flow in a tube with a sharp inlet edge over the reduced length range  $X/d = 0.1-13$  at  $Re_d = (13-110) \cdot 10^3$ , which corresponds to mean flowrate velocities of 5.5-46 m/sec.

Experiments were carried out on a stand with a cross section 36 mm in diameter, described in [3]. A flow-type calorimeter with seven built-in heat flux sensors [4] was used for  $X/d \geq 0.4$ . The arrangement of the stand with the flow-type calorimeter is shown in Fig. 1a. Water, boiling in the cavity of the casing of linear segment 5 is pumped by micropump 3 through the jacket of calorimeter 1 and the annular chamber of inlet flange 2. The water flowrate was regulated so that its temperature drop in the tube circuit would not exceed 1 K and the regime  $T_w = \text{const}$  would be kept at 369-371 K. The axial coordinates of the sensors were varied by placing heated inserts of length  $\Delta X = 6$  and 12.5 mm in the joint between the inlet flange and the calorimeter or linear segments 4 of length  $l = 100$  or 200 mm in the same joint. The design of the inserts is shown in Fig. 1b. Measurement results obtained using the heat flux sensors were processed according to the recommendations of [5] and had an error of  $\pm 10\%$ .

For  $X/d < 0.9$  the local heat transfer intensity was determined by the method described in [6]. Instead of the flow-type calorimeter, a working segment, whose design is shown in Fig. 1c, was connected with the stand inlet. Its cylindrical active part, held in the necks of textolite 1 and steel 2 flanges, was made from the compound UP592-11, which retains its mechanical properties up to temperatures of 420-430 K [7]. First, a round billet ( $d_{in}/d_{out} = 36/50$  mm/mm) was manufactured by permanent-mold casting. Then, the outer diameter of the billet was turned down to a diameter of 37 mm, and 13 copper-constantan thermocouples having wires 0.1 mm in diameter were glued to the thin-walled jacket obtained. The thin-walled jacket equipped with the thermocouples was placed in the same mold,

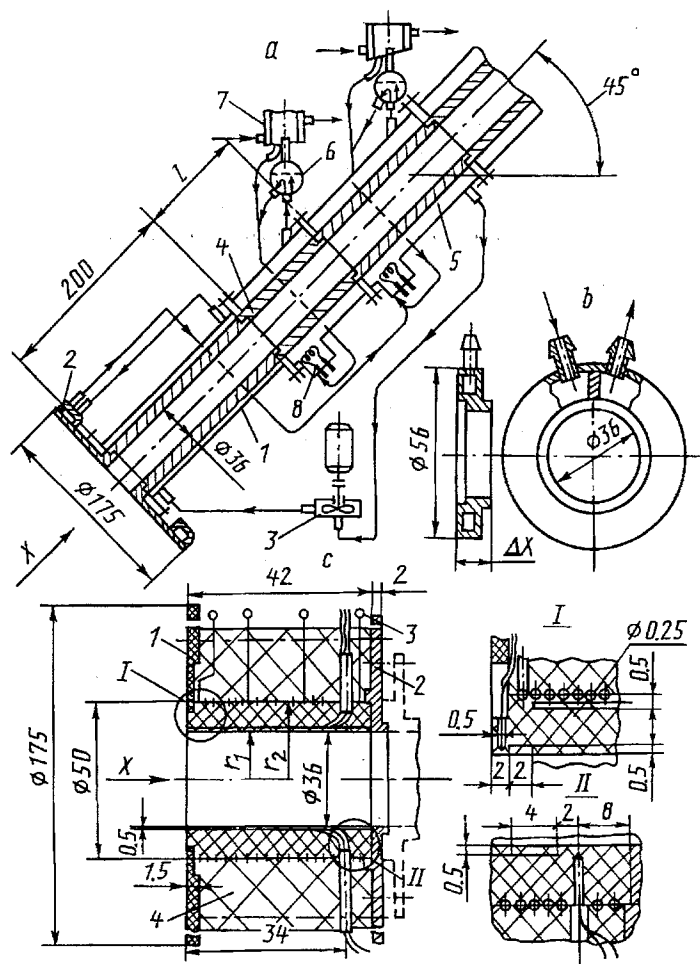


Fig. 1. Arrangement of the experimental set-up: a) entrance segment with a flow-type calorimeter: 1) calorimeter; 2) heated inlet flange; 3) water pump; 4, 5) linear segments; 6) separator; 7) condenser; 8) electric heater; b) heated insert; c) entrance segment for determining the local heat transfer coefficients by the gradient method: 1, 2) inlet and connecting flanges; 3) electric heater; 4) thermal insulation.

and the original outer diameter of the working section was restored by a second casting of the compound. Electric heater 3 was wound in a threaded groove with a pitch of 0.3 mm and consisted of three independent sections supplied from dc sources. Thermocouples recording the heated surface temperature were located in the grooves beneath the electric heater. The wall temperature of the working segment was monitored in the radial direction by three thermocouples at its inlet face and by three thermocouples in drilled holes at a distance of 34 mm from the inlet edge. Two thermocouples were glued at the inner and outer boundaries of thermal insulation layer 4. During the measurements the wall temperature of the working segment on the heat removal side was kept constant along X at 369-371 K. Heat losses to the surrounding medium did not exceed 2%.

Measurements with the IT-2 device yielded a thermal conductivity of the pure compound of  $\lambda = 0.43$  W/(m·K) [8], and within the range 290-380 K the dependence  $\lambda = f(T)$  proved insignificant. The effective thermal conductivity of the material of the wall with built-in thermocouples was estimated from calibration experiments under natural convection by Eq. (1). It amounted to  $\lambda = 0.8$  W/(mK) with an error of  $\pm 8\%$  at a confidence probability of 0.95:

$$\lambda = \frac{q_l \ln r_2/r_1}{2\pi(T_2 - T_1)}. \quad (1)$$

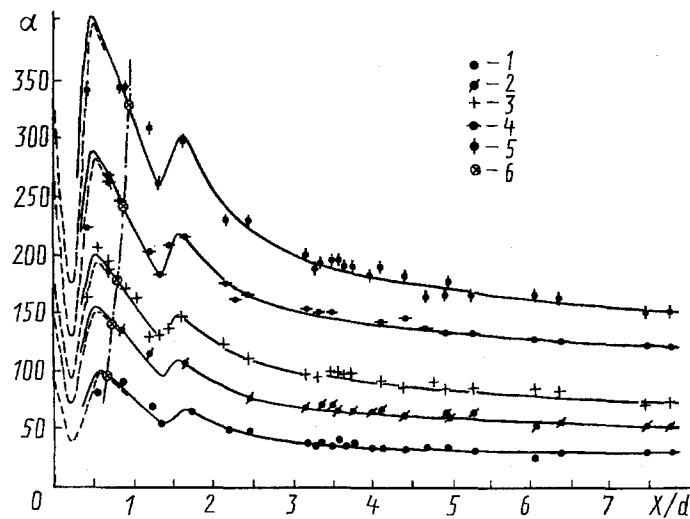


Fig. 2. Distribution of the local heat transfer coefficients  $\alpha$ , W/(m<sup>2</sup>·K), along the entrance segment: 1)  $Re_d = 13 \cdot 10^3$ ; 2)  $28 \cdot 10^3$ ; 3)  $42 \cdot 10^3$ ; 4)  $77 \cdot 10^3$ ; 5)  $Re_d = 110 \cdot 10^3$ ; 6) by formula (8).

Under forced convection, the longitudinal distributions of the local heat transfer coefficients were found by solving differential heat conduction equation (2). Following [6], boundary conditions (3)-(5) were assigned using temperature measurements, and unknown boundary condition (6) was chosen by successive approximations so that predicted and measured temperatures of an inner surface would agree with a given accuracy

$$\frac{\partial^2 T}{\partial r^2} + \frac{1}{r} \frac{\partial T}{\partial r} + \frac{\partial^2 T}{\partial X^2} = 0, \quad (2)$$

$$T|_{x=0} = T_{x=0}(r), \quad (3)$$

$$T|_{x=x_1} = T_{x_1}(r), \quad (4)$$

$$T|_{r=r_2} = T_{r_2}(X), \quad (5)$$

$$\alpha|_{r=r_1} = \alpha_{r_1}(X) \quad (6)$$

(trial-and-error method). The final discrepancy in temperature was taken equal to 0.5 K. An ES-1061 computer was used for solution by the net method with a net step of 1 mm in the radial direction and 2 mm along the X-axis. To find the roots of the equivalent system of linear algebraic equations the Gauss method was used with the choice of the basic element [9]. This reduced the sensitivity toward rounding off errors. The final error in determining the local heat transfer coefficients amounted to  $\pm 22\%$ .

Graphs combining the experimental results of both runs are shown in Fig. 2. The dashed lines are results obtained by the gradient method. The distributions  $\alpha = f(X/d)$  have a minimum near the input edge and two maxima downstream. Stabilization of the heat transfer coefficients starts in the region  $X/d > 7.5$ , where their values correspond to the following formula [10]<sup>\*</sup> with a deviation of no more than 5%:

$$Nu_d = 0,022 Re_d^{0,8} Pr^{0,43}. \quad (7)$$

The extrema are almost stationary over the considered ranges of  $Re_d$ . In this case, a minimum lies not in the stagnation region as would be expected from visualized observations [2], but in the cross section  $X/d = 0.22$  somewhat ahead of the far edge of a small-size vortex. At the minimum the local values of  $\alpha$  remain 20-30% higher than in developed flow, and the next, in essence jumpwise, increase in heat transfer by 130-150% takes place on a very small (0.3-0.35 diameter) segment of the tube. The second maximum results from the transient process in the laminar boundary

\* Some of the experimental data for  $X/d > 7.5$  are plotted in Fig.4.

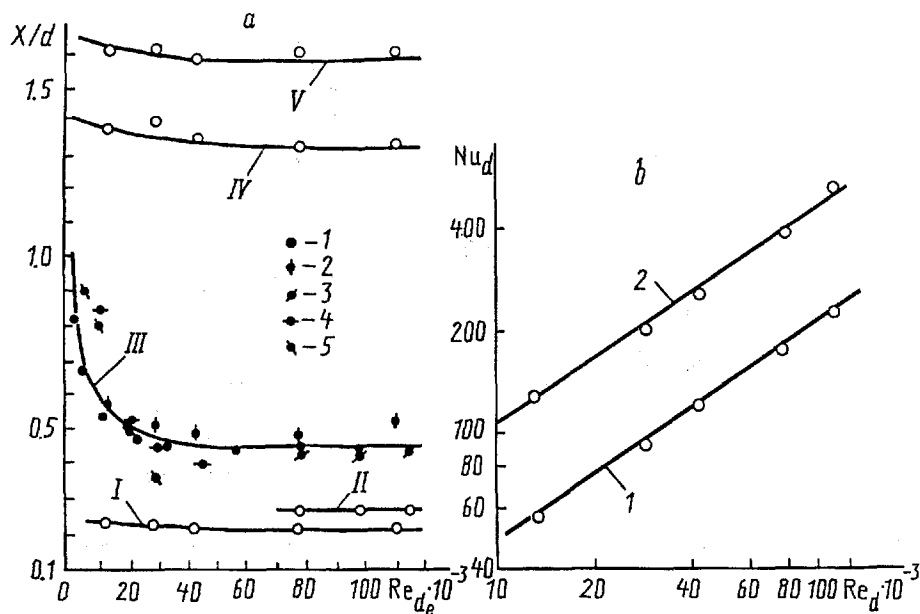


Fig. 3. Location parameters and heat transfer intensity vs Reynolds number for characteristic cross sections on the entrance segment: a: I) minimum of the heat transfer coefficients; II) vortex edge; III) global maximum of heat transfer coefficients: 1) according to [13]; 2) according to Fig. 2; 3) according to [12]; 4) according to [15]; 5) according to [14]; IV and V) beginning and end of the transition region; b: 1) minimum of the heat transfer coefficients; 2) global maximum of the heat transfer coefficients.

layer. From Fig. 2 it is seen that the critical coordinates for transition practically do not depend on  $Re_d$ , and the usual conditions  $R_{xcr}^I = \text{const}$ ,  $R_{xcr}^{II} = \text{const}$  for nonseparated flows are not satisfied. The latter should not be considered unexpected since in [11] it has been found that on the entrance segments of channels having leading edges profiled by circles of small radii  $R/d = 0.125-0.5$  the transition region is increasingly shifted downstream with increase in  $Re_d$  and the quantities  $R_{xcr}^I$  and  $R_{xcr}^{II}$  are no longer constant. The dash-dot line in Fig. 2 denotes the location of cross sections with a zero velocity at the wall. Their coordinates are calculated by formula (8) taken from [12]. No any specific features associated with the above cross sections are revealed in the configuration of the distributions  $\alpha = f(X/d)$ :

$$(X/d)_0 = 0,115 Re_d^{0,18}. \quad (8)$$

The coordinates of the extrema of local heat transfer on the entrance segment of a tube with a sharp inlet edge are shown in Fig. 3a. Curve III, pertaining to the global maximum, was calculated using an equation approximating the data in Fig. 2 and those from [13-15] within the range of  $Re_{de} = (3-110) \cdot 10^3$ :

$$(X/d_0)_{\max} = 0,46 + \frac{10^3}{Re_{d_0}}. \quad (9)$$

Curve II for the cross section in which the far edge of the vortex is located, is constructed using the data in [2]. The relation  $Nu_d = f(Re_d)$  at a minimum and in the cross section of a global maximum is shown in Fig. 3b and is governed by the equations

$$Nu_d^{\min} = 0,108 Re_d^{0,66}, \quad (10)$$

$$Nu_d^{\max} = 0,252 Re_d^{0,66}. \quad (11)$$

Since the distributions  $\alpha = f(X/d)$  incorporate structural components with a laminar heat transfer regime, the experimental results are processed in dimensionless form in Fig. 4 in the system of similarity parameters  $[Nu_d; 1/Pe X/d]$ . Just as in Fig. 2, the dashed line identifies a region where heat transfer coefficients have been determined

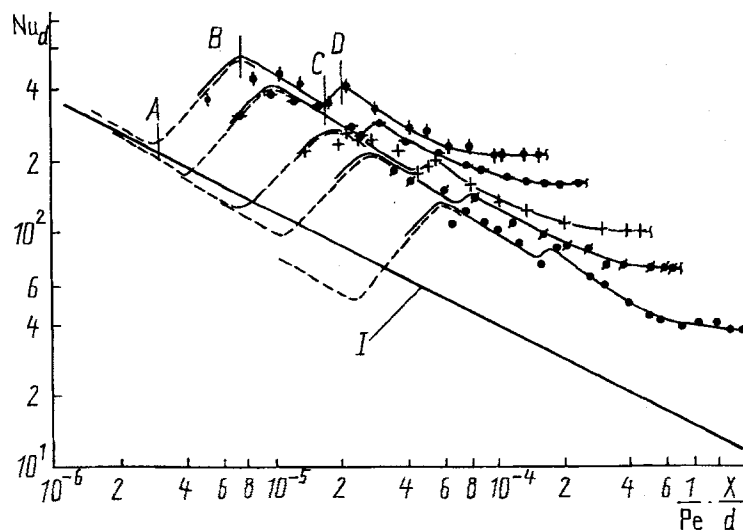


Fig. 4. Dimensionless processing of the experimental data: I) by formula (12). The symbols are the same as in Fig. 2.

by the gradient method. In the upper graph for  $Re_d = 110 \cdot 10^3$  a heat transfer intensity minimum A, a global maximum B, transition region edges C and D are indicated. On the left, the limiting Nusselt numbers refer to the reduced length  $X/d = 0.1$  because of a possible incorrectness of the local heat transfer coefficients calculated by the gradient method near the inlet edge, where it is necessary to resort to an extrapolated estimate of the temperature state of the surface in the cross section  $X/d = 0$ . Curve I corresponds to the equation for the case of a nonseparated laminar flow in the boundary layer of the entrance segment and for  $Re_d > 10^4$  [16]:

$$Nu_d = 0,381 \left( \frac{1}{Pe} \frac{X}{d} \right)^{-0,5} + 2,3. \quad (12)$$

The graphs of  $Nu_d = f(1/Pe \cdot x/d)$  for constant Reynolds numbers are identical in shape and are quite satisfactorily linearized inside the components of their fragments up to the end of transition region D. Ahead of minimum A and on the segment B-C that precedes beginning of the transition, a slope of the averaging lines is  $m = -0.55$ , which is correlated with values characterizing the specific features of heat transfer in laminar flows, especially if the flow counter to the core near a minimum and the existence of a velocity discontinuity in the boundary layer beyond global maximum B are taken into account. On segment A-B the slope is  $m = +1$ . The local Nusselt numbers in the stagnation region adjacent to the input edge and beneath the vortex close to minimum A are near curve I regardless of the specific features of the velocity profiles. Only at  $Re_d = 13 \cdot 10^3$  are the discrepancies above 25%. However, beyond maximum B, where secondary laminar flow starts, the  $Nu_d$  numbers lie much higher, deviating from curve I by 150-250%.

A computational scheme for the local heat transfer coefficients ahead of a minimum and on segments A-B and B-C must be constructed by using the similarity-type number relation  $Nu_d = cRe_d^n(1/Pe \cdot X/d)^m$  because of the diversity of the graphs  $Nu_d = f(1/Pe \cdot X/d)$  according to the Reynolds number. Analysis yields the following relations:

$$\text{at } 0,1 < X/d < (X/d)_{\min} \quad Nu_d = 0,06 Re_d^{0,11} \left( \frac{1}{Pe} \frac{X}{d} \right)^{-0,55}, \quad (13)$$

$$\text{at } (X/d)_{\min} < X/d < (X/d)_{\max} \quad Nu_d = 0,355 Re_d^{1,66} \left( \frac{1}{Pe} \frac{X}{d} \right), \quad (14)$$

$$\text{at } (X/d)_{\max} < X/d < (X/d)_{kp}^I \quad Nu_d = 0,215 Re_d^{0,11} \left( \frac{1}{Pe} \frac{X}{d} \right)^{-0,55}. \quad (15)$$

Upon substituting  $Pe = RePr$  and  $Pr = 0.71$ , Eqs. (13)-(15) assume the form:

$$\text{at } 0,1 < X/d < (X/d)_{\min} \quad Nu_d = 0,049 Re_d^{0,66} (X/d)^{-0,55}, \quad (16)$$

$$\text{at } (X/d)_{\min} < X/d < (X/d)_{\max} \quad Nu_d = 0,5 Re_d^{0,66} (X/d), \quad (17)$$

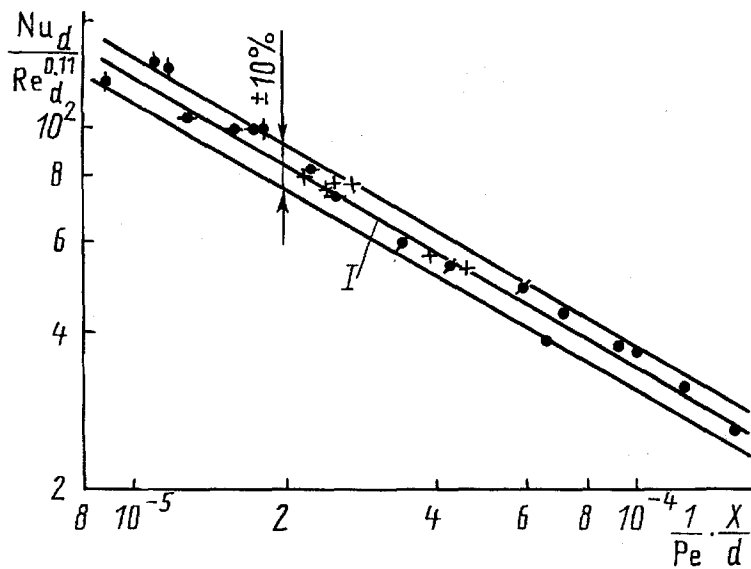


Fig. 5. Generalization of the experimental data on the local heat transfer on the portions of the entrance segment between a global maximum and the beginning of a transition (B-C in Fig. 4): I) by formula (15). The symbols are the same as those in Fig. 2.

$$\text{at } (X/d)_{\max} < X/d < (X/d)_{\text{kp}}^1 \quad Nu_d = 0,178 Re_d^{0,66} (X/d)^{-0,55}. \quad (18)$$

Coincidence of exponents of the Reynolds number in Eqs. (16)-(18) enables one to assume that countercurrent laminar flow in a boundary layer is retained beneath the vortex and even in some part of the stagnation region, and the increase in the local heat transfer intensity ahead of a minimum is the cause of the sharp decrease in the thickness of the film of countercurrent flow to the left of cross section A. Equations (16)-(18) agree with experiment with an error  $\pm 10\%$ . When the coordinates of the minimum (Fig. 3) and the global maximum of the local heat transfer coefficients (Eq. (9)) are substituted into the latter equations, the calculated  $Nu_d^{\min}$  numbers prove to be 10-12% less, and the  $Nu_d^{\max}$  numbers 10-12% higher, than those in Eqs. (10) and (11) since the graphs of  $Nu_d = f(1/Pe \cdot X/d)$  become nonlinear in the immediate vicinity of extrema. A generalization of the experimental Nusselt numbers on segment B-C (see Fig. 4) between a global maximum and the beginning of a transition based on Eq. (15) is shown in Fig. 5.

In conclusion, we note that the laws of local heat transfer on the entrance segment of a smooth tube with a sharp inlet edge, supporting as a whole the physical model of [2], indicate that the boundary layer in a separated flow region, just as in nonseparated mixed flows, alternately passes through laminar, transient, and turbulent stages when  $Re_d > 10^4$ . In this case, a minimum and a global maximum of the heat transfer coefficients accompany the first of the mentioned stages involving laminar boundary layer flow.

## NOTATION

$X$ , longitudinal coordinate, mm;  $\Delta X$ , length of the insert, mm;  $l$ , length of the linear section, mm;  $d$ , diameter of the flow-type part of the stand, mm;  $r_1$ , radius of the inner tube surface, mm;  $r_2$ , radius of the outer tube surface, mm;  $\lambda$ , thermal conductivity of the compound, W/(m·K);  $T$ , temperature, K;  $\alpha$ , local heat transfer coefficient, W/(m<sup>2</sup>·K);  $Nu_d$ , Nusselt number;  $Re_d$ , Reynolds number;  $Pe$ , Peclet number;  $Pr$ , Prandtl number. Subscripts and superscripts: max, maximum; min, minimum; e, equivalent; cr, critical; I, II, first and second critical values.

## REFERENCES

1. G. Grass, Allgemeine Wärmetechnik, 7, No. 3, 58-64 (1956).

2. V. M. Legkii and V. A. Rogachev, *Inzh.-Fiz. Zh.*, **56**, No. 2, 215-220 (1989).
3. V. M. Legkii and V. D. Burlei, *Teploénergetika*, No. 9, 86-88 (1976).
4. V. M. Legkii and V. D. Burlei, *Prom. Teplotekhnika*, **1**, No. 1, 6-9 (1985).
5. V. M. Legkii, O. A. Gerashchenko, and V. D. Burlei, *Teplofiz. Teplotekhn.*, Issue 34, 9-12 (1978).
6. L. A. Kozdoba and P. G. Krukovskii, *Methods of Solving Inverse Heat Conduction Problems [in Russian]*, Kiev (1982).
7. *Handbook on Plastic Masses [in Russian]*, Vol. 2, Moscow (1975).
8. E. S. Platunov, S. E. Buravoi, V. V. Kurepin, and G. S. Petrov, *Thermophysical Measurements and Devices [in Russian]*, Leningrad (1986).
9. E. A. Volkov, *Numerical Methods [in Russian]*, Moscow (1987).
10. V. A. Mukhin, A. S. Sukomel, and V. N. Velichko, *Inzh.-Fiz. Zh.*, **5**, No. 11, 3-7 (1962).
11. V. M. Legkii and A. S. Makarov, *Teplofiz. Teplotekhn.*, Issue 20, 106-112 (1971).
12. V. M. Legkii and V. A. Rogachev, *Inzh.-Fiz. Zh.*, **56**, No. 4, 547-550 (1989).
13. A. S. Makarov, "Some laws of flow and heat transfer on entrance segments of rectangular channels," *Dissertation*, Kiev (1970).
14. E. M. Sparrow and N. Car, *Teploperedacha*, **105**, No. 3, 100-109 (1983).
15. E. M. Sparrow and N. Car, *Teploperedacha*, **104**, No. 1, 89-97 (1982).
16. V. M. Legkii, *Inzh.-Fiz. Zh.*, **34**, No. 4, 581-588 (1978).